Advanced Spectroscopic Approachs for Assessing the aging level for Zirconium-based Pyrotechnic Initiator

Ji-Hoon Ryu, Jun-Ho Yang, Jack J. Yoh
Department of Mechanical and Aerospace Engineering, Seoul National University
Seoul, Korea 151-742

1 Introduction

Solid mixtures have long been used as pyrotechnic materials in military or private sectors due to its high energy through instant combustion. Owing to its explosive characteristic in powder form, zirconium (Zr) is mixed with an oxidizing agent such as potassium perchlorate ($KClO_4$) to achieve excellent combustion performance [1]. However, over a long period of storage, the material undergoes a process termed as aging that accompanies changes in activation energy and heat of enthalpy [2]. Continuous aging can cause combustion failures such as misfires that deviates from the intended performance. Therefore, it is important to understand exactly the degree of aging process for pyrotechnic materials.

Laser-induced breakdown spectroscopy (LIBS) is a useful spectroscopic technique for atomic detection that can obtain spectral information of the emitted light from plasma. LIBS require only a small amounts of sample without any chemical preprocessing for component identification. Furthermore, LIBS is useful for a wide range of applications because of its high detection sensitivity, distant analysis, and real-time analysis [3]. The spectral information of the emitted plasma is provided differently depending on the atom and molecule from electromagnetic, vibrational, and rotational transitions. Molecules constitute the interatomic distance through combination of various forms between elements. Here, the spectra of molecules have a distinct identity at wavelengths different from constituent atoms, providing distinguishable information from an atomic signal. Meanwhile, x-ray photoelectron spectroscopy (XPS) investigates a material by obtaining the inherent binding energy of each component from photoelectron kinetic energy by photoelectric effect. From the information on chemical state, XPS enables for qualitative and quantitative analysis of the material.

This study is aimed to estimate the thermal performance of pyrotechnic initiator ($Zr/KClO_4$), which is composed of Zr fuel and $KClO_4$ oxidant, according to hygro-thermal aging through spectroscopic analyzes. LIBS and XPS studies were performed on accelerated aged samples under various humidity and heat conditions. In LIBS study, the oxidation level of Zr was determined based on the difference in ZrO molecular signal relative to the amount of ZrO_2. Meanwhile, the decomposition amount of $KClO_4$ into $KClO_3$ and KCl with respect to aging was determined by quantitative XPS analysis. Then, NASA CEA (chemical equilibrium with application) code was used to predict the thermal performance based on composition, which is estimated from spectral analyzes. In addition, we verify the feasibility of spectroscopic analysis results with DSC experiments. Performance prediction technique based on spectroscopic analyzes has been proposed to determine the performance of pyrotechnic materials.

Correspondence to: jjyoh@snu.ac.kr

2 Experimental setup

2.1 LIBS setup

The LIBS system uses a Q-switched Nd:YAG laser (RT250-Ec, Applied Spectra Inc.) at 1064 nm with a pulse duration of 5 ns at 30 mJ of energy (3.82×10^{12} W/m^2). The laser beam is passed through a beam expander to reduce the divergence of the beam area, and focused with a 15x magnification objective (LMM-15X-P01, Thorlabs) to generate a beam without introducing chromatic aberration. The focal distance can be adjusted by moving the position of sample on a xyz-stage. Also, the incremental spot locations (at 1 mm apart) are chosen be larger than a single beam spot size (about 100 μm) to minimize the effect of ablation and maintain constant focal length, a thermal effect. Furthermore, a six-channel CCD spectrometer is set to detect the plasma in wavelength range from 198 to 1050 nm. The spectral resolution of the CCD is classified to about 0.1 nm for ultraviolet (UV) to visible (VIS) wavelengths and 0.12 nm for visible to near-infrared (NIR) wavelengths at 13,000 wavelength channels. The gate width and laser repetition rate are fixed at 1.05 ms and 1 Hz, respectively. The gate delay is set at 1.0 μs considering the reference.

2.2 XPS setup

Chemical information about the material has been obtained through a commercial XPS equipment (AXIS SUPRA instrument, Kratos analytical Ltd., U.K.). The spectrometer was equipped with an automated monochromatic aluminum Kα X-ray sources (hν = 1486.6 eV), and an energy resolution of less than 0.48 eV. The XPS spectrum was constructed on a highly sensitive hemispherical electron energy analyzer (WX-600) composed of several individual data channels. The analyte can be freely positioned in ultrahigh vacuum (UHV) chamber through x, y and z directions, and θ, Φ rotations. The chamber pressures for sample and load-lock were set to 5×10^{-10} and 5×10^{-8} torr, respectively, under the experimental conditions.

2.3 DSC setup

Calorimetric analysis was performed at 50 - 650 °C to evaluate the heat of reaction from chemical reaction between Zr and $KClO_4$ through differential scanning calorimetry (DSC, Mettler Toledo Inc., DSC 3 model). DSC curves were collected on the basis of ICTAC (International Confederation for Thermal Analysis and Calorimetry) standards on notation. Each 2.00 mg sample powder was prepared in a standard pierced aluminum pan with a diameter of 40 μm. The experiment was carried out at a heating rate of 10 °C/min in nitrogen atmosphere of 80 ml/min.

2.4 Sample preparation

Table 1 represents the details of Zr/$KClO_4$ samples. Basic material compositions were Zr (53 %), $KClO_4$ (42 %), Viton-b (5 %). The aged samples were obtained by monitoring the aging duration related to oxidation process. Hygro-thermal aging condition (both heat and moisture) was set to 71 °C with relative humidity of 70 %. On the other hand, in LIBS study, non-aged samples mixed with ZrO_2 have been used to draw a calibration curve with different concentrations of Zr and ZrO_2 in the Zr composition of each material.

Table. 1. Details of $Zr/KClO_4$ samples

		Composition of non-aging samples (%)	Aging conditions
$Zr/KClO_4$	Zr	53x *	Hygrothermal aging for 2, 4, 8, 16 weeks
	ZrO_2	53(1-x)	
	$KClO_4$	42	
	Viton-b	5	

[*] : x indicates $Zr/(Zr+ZrO_2)$ ratio, which is ranged from 0.2 to 1.0.

3 Results

3.1 LIBS analysis

In this study, we utilized the effect of Zr and ZrO_2 concentration on ZrO signal generation. Figure 1(a) shows the spectrum for ZrO molecular signal of $Zr/KClO_4$. The experiments were carried out on non-aged samples mixed with ZrO_2 and also on aged samples. The emission spectra of ZrO signal corresponding to a wavelength range of about 623 to 660 nm were remarkably observed with a unique band structure. The emission of ZrO molecular band signal appears in the form of an intermediate in both Zr and ZrO_2. However, we estimated that under the same experimental conditions, the emission of ZrO signal would occur differently in two sources. Meanwhile, a certain amount of ZrO signal is expected even at a high concentration of Zr due to the recombination of Zr and oxygen in air during the cooling process. These results show that ZrO band signal is generated in both Zr-based elements, but the signal intensity per weight is more dominant in ZrO_2. For aged samples, increasing signal intensity is observed with aging duration in Fig. 1(b). In addition, it follows closely an increasing trend of non-aged samples with added ZrO_2. Figure 2 shows the data processing results of ZrO α (1,0) bands of the $b^3\phi - a^3\Delta$ system over time. To quantify the content of ZrO_2 in the material, an AUC (area under the curve) method was applied to ZrO band signal by integrating the related band region in Fig. 1.

In this study, we set pure binder as a background for AUC calculations due to its inactive characteristics in LIBS. Data processing was performed using OriginPro software (OriginLab, OriginPro 8.5.1, USA). The ZrO_2 concentration (x) and corresponding area under the band structure (y) is expressed by the equation ($y=270\,x + 6439$) with a correlation coefficient of $R^2 = 0.93$. As time period increases, it is clear that aged $Zr/KClO_4$ follows the behavior of non-aged samples with increasing ZrO_2 concentration. The weight concentration of Zr and ZrO_2 with respect to whole substance are shown in Fig. 2(b). The graph clearly shows a decrease in Zr and an increase in ZrO_2 with both samples. The concentration of ZrO_2 were estimated to be about 23.1%, 33.2%, 38.3% and 41.4% with respect to aging steps. By using AUC results of the ZrO band, we have demonstrated a method for predicting the concentration of oxidation of Zr in aged pyrotechnic samples. As a result, it is clearly confirmed that the oxidation level of Zr increases over time. In conclusion, these results indicate that the oxidation of Zr is closely related to the aging process of Zr-based pyrotechnic materials.

Oxidation of Zr fuel over time has resulted due to following reasons. In general, a high electron affinity of Zr causes a molecule product with oxygen, which is adsorbed on the surface as a thin oxide film. After that, the oxide layer thickness composed of ZrO_2 gradually increases as aging time is increased. Moreover, this tendency is further accelerated by the presence of humidity and oxidants, which significantly degrades the explosive performance of Zr-containing ignition devices [4]. Furthermore, hydrogen-induced cracking can occur from hydrogenation environment, which is formed under high moisture conditions, resulting in increased surface area and increased oxidation [5].

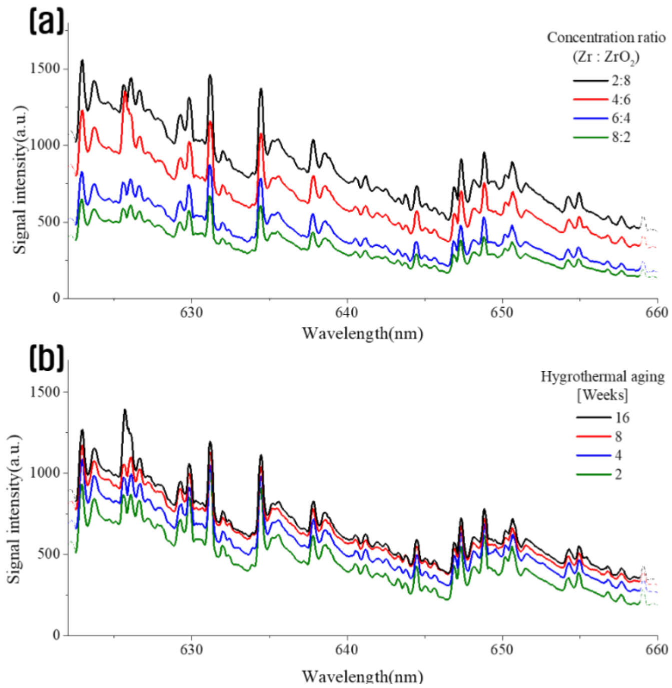

Fig. 1. The emission spectra for Zr/KClO4. (a) non-aging samples with added ZrO2, (b) hygrothermal aging samples.

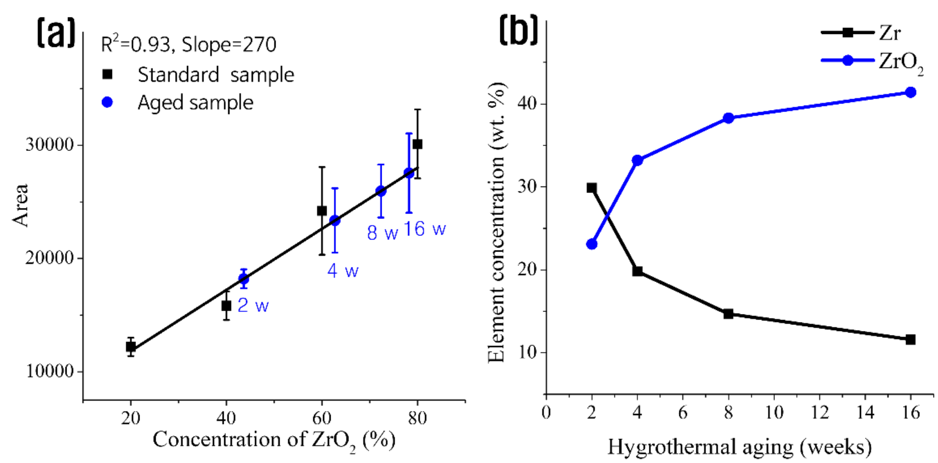

Fig. 2. Data processing results for ZrO emission spectra of LIBS; (a) calibration curve, and (b) estimated amount of Zr oxidation

3.2 Quantitative XPS analysis

Figure 3 shows the spectral results of XPS according to hygro-thermal aging level. As expected, it is clearly demonstrated that the oxidation of Zr shows the same tendency as LIBS results. On the other hand, $KClO_4$ is decomposed into small amount of $KClO_3$ and large amount of KCl as exposed to moisture and heat. Here, the decomposition of $KClO_4$ can be attributed to weak bonding of Cl-O or the redox reaction with metal fuels under moisture-rich conditions [6, 7].

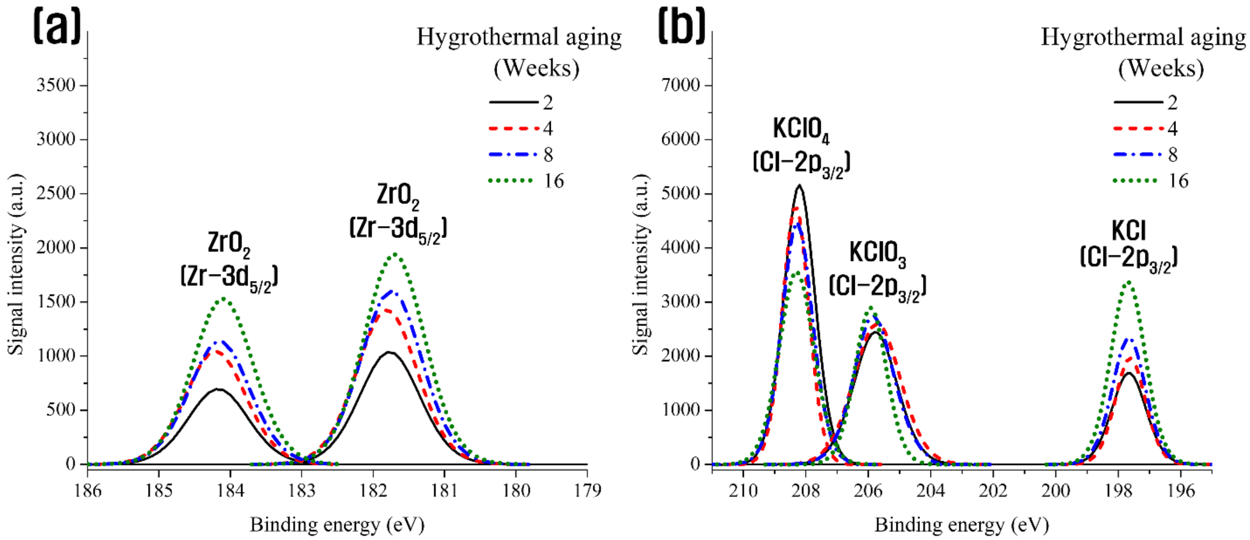

Fig. 3. XPS results of (a) ZrO_2 and (b) $KClO_4$ for Zr/$KClO_4$ according to the degree of hygrothermal aging.

3.3 Estimation of thermal performance based on spectral analysis.

From spectroscopic results, we have predicted the thermal performance by determining the content of material with aging. The heat of reaction, one of the key properties for evaluating the performance of pyrotechnic materials, was calculated by using the NASA CEA code. Here, the content of components was estimated by LIBS analysis for fuel-related elements and quantitative XPS analysis for oxidant-related elements, respectively. Table 2 shows content of materials according to different hydrothermal aging level. In order to verify the validity of heat of reaction value through spectroscopic analysis, calorimetric analysis for samples under the same conditions was carried out by DSC experiment. Figure 4 compares the heat of reaction results obtained from spectroscopic analysis (CEA) and calorimetric analysis (DSC). Here, DSC measured less due to non-ideal experimental conditions, incomplete combustion, and absorption of heat from non-chemically reacting elements. However, on the whole, the heat of reaction shows a decreasing tendency in both results as aging progresses, which suggests that the spectroscopic analysis can be a useful tool for interpreting thermal performance of energetic materials.

Table. 2. The constituent content of Zr/$KClO_4$ with aging

	2 weeks	**4 weeks**	**8 weeks**	**16 weeks**
Zr	29.90	19.80	14.70	11.60
ZrO_2	23.10	33.20	38.30	41.40
$KClO_4$	23.34	21.42	19.69	15.22
$KClO_3$	11.04	11.78	12.07	12.36
KCl	7.62	8.80	10.24	14.42
Viton-b	5.00	5.00	5.00	5.00

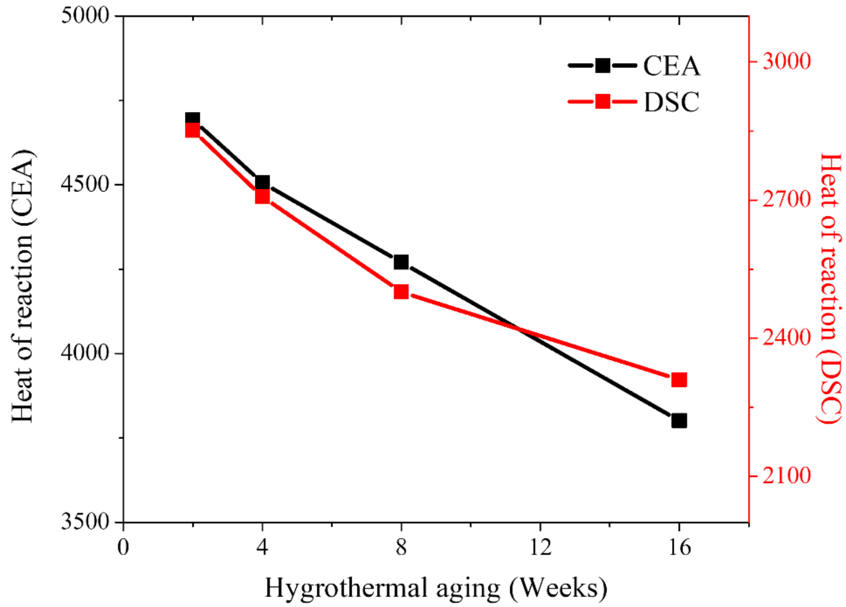

Fig. 4. Comparison of CEA and DSC results for heat of reaction according to degree of hygrothermal aging.

ACKNOWLEDGMENTS

This work was financially supported by Korea National Research Foundation under the National Space Laboratory Program 2014 (NRF-2014M1A3A3A02034903) and the Basic Science Research Program 2016 (NRF-2016R1D1A1A02937421) through IAAT at Seoul National University. Additional support was provided by the Hanwha Yeosu Grant 2018.

References

[1] Agrawal JP. (2010). High Energy Materials: Propellants, Explosives and Pyrotechnics. Wiley-VCH. Weinhein.

[2] Sorensen DN, Quebral AP, Baroody EE, and Sanborn WB (2006). Investigation of the thermal degradation of the aged pyrotechnic titanium hydride/potassium perchlorate. J. Therm. Anal. Calorim. 85(1): 151

[3] Musazzi SZ, Perini U. (2014). Laser-induced breakdown spectroscopy: Theory and applications. Springer. Press. Berlin. Germany.

[4] Lyapin A, Jeurgens LPH, Graat PCJ, and Mittemeijer EJ. (2004). The initial, thermal oxidation of zirconium at room temperature, J. Appl. Phys. 96: 7126.

[5] Gao SJ, Simmons GW, and Wei RP. (1984). Fatigue crack growth surface reactions for titanium alloys exposed to water vapor. Mater. Sci. Eng. C. 62: 65

[6] Armando B, Juan A, Stephane N, and Bernard S. (1999). Structure and Bonding of Chlorine Oxides and Peroxides: ClO_x, ClO_{x-} (x=1-4) and Cl_2O_x (x=1-8), J. Phys. Chem. 103(16): 3078.

[7] Hori H, Kamijo A, Inoue M, Chino A, Wu Q, and Kannan K. (2018). Efficient decomposition of perchlorate to chloride ions in subcritical water by use of steel slag. Environ. Sci. Pollut. R. 25(8): 7262.